

Effect of ionic substitutions on the structure and dielectric properties of hafnia: A first principles study

Eric Cockayne^{a)}

Ceramics Division, Materials Science and Engineering Laboratory, National Institute of Standards and Technology, Gaithersburg, Maryland 20899-8520, USA

(Received 13 November 2007; accepted 6 February 2008; published online 18 April 2008)

First principles calculations were used to study the effects of Si, Ti, Zr, and Ta (+N) substitutional impurities on the structure and dielectric properties of crystalline HfO₂. The dielectric constant of monoclinic HfO₂ can be enhanced by substituting more polarizable ions for Hf, but the band gap is decreased. Enhancing the permittivity without decreasing the band gap requires forming the tetragonal or cubic phase of HfO₂. Among the ions studied, Si alone is found to stabilize a nonmonoclinic phase of HfO₂ relative to the monoclinic phase, but only at an atomic concentration above about 20%. Various experiments have reported the formation of nonmonoclinic phases of HfO₂ with increased permittivity when other ions are substituted for Hf. It is concluded that these structures are, in general, either metastable or are stabilized by extrinsic factors or by a layered arrangement of the substitutional cations. © 2008 American Institute of Physics.

[DOI: [10.1063/1.2903870](https://doi.org/10.1063/1.2903870)]

I. INTRODUCTION

The properties of HfO₂, including the fact that it has a higher static dielectric permittivity κ_s than SiO₂, make it one of the leading candidates for an alternate gate dielectric material.^{1–3} In addition to having a high permittivity, a practical gate dielectric material must exhibit phase stability in contact with Si, have low leakage current, have appropriate band offsets and threshold voltage stability, and maintain sufficient channel electron and hole mobility, etc. Drawbacks with HfO₂ as a gate dielectric material include an unstable threshold voltage and low channel mobility.

It is natural to attempt to improve the properties of HfO₂ by the substitutional addition, or “doping,” of different ions. Improved properties have been reported with the addition of Al,⁴ Y,^{5,6} La,⁷ other rare earth elements,⁸ Si,⁹ Ti,¹⁰ Zr,¹¹ and Ta plus N.¹² Generally, the reports show higher threshold stability, implying fewer charge trapping defects, while maintaining a sufficiently low leakage current. Furthermore, numerous studies show that κ_s can be substantially increased, from roughly 15 to roughly 30 by the addition of other ions and appropriate heat treatment.^{4–6,8,9} Substitutional addition of other ions to HfO₂ is thus a promising avenue to practical gate dielectrics for advanced semiconductor applications.

Pure HfO₂ has three polymorphs as a function of temperature (Fig. 1). At high temperatures, it has the cubic fluorite structure with the Hf coordinated with a cube of eight O and the O coordinated with a tetrahedron of four Hf; at intermediate temperatures, a tetragonal distorted fluorite structure, and at low temperatures, a monoclinic phase with the Hf sevenfold coordinated, half of the O fourfold coordinated and half threefold coordinated. The phase transformation between tetragonal and monoclinic is first order by symmetry. The phase transformation between cubic and tetragonal order

is also first order, although it is not constrained to be so by symmetry. In those experiments where the permittivity of HfO₂ is enhanced by doping, the increase in κ_s is always associated with a change of symmetry from the monoclinic phase of HfO₂ to the tetragonal or cubic one.

The most stable phases (or two-phase mixtures) for HfO₂ with ionic substitutions are given in the published equilibrium phase diagrams.¹³ The maximum solubilities of the above-mentioned ions in the low-temperature monoclinic HfO₂ structure are given in Table I. Except for ZrO₂, which is isostructural with HfO₂, the solubilities are generally small (order 1%–10%) and decrease with decreasing temperature. Table II contains one oxynitride, TaON. This structure has not been studied much, but it is essentially isostructural with HfO₂ (Fig. 2) except that the N all go on the fourfold oxygen sites of HfO₂.¹⁴ Given the structural similarities between HfO₂ and TaON, it is quite possible that they form a complete solid solution series.

Contrast that with the experimental results showing (1) much greater concentrations of dopants in HfO₂ than is possible under thermodynamic equilibrium and (2) the formation of phases other than monoclinic, such as amorphous structures and higher-permittivity tetragonal or cubic phase of HfO₂. Given that these oxides are typically deposited at room temperature and annealed at temperatures no higher than 1000 °C, it is likely that compositionally metastable structures are being produced. As the familiar examples of glass and diamond show, however, metastability of a structure does not preclude its usefulness, provided that the barriers to decomposition or structural transformation are sufficiently large to prevent the structure from transforming over the lifetime of the device in which it is used.

First principles calculations provide tools for exploring the relative stability of different structures and for calculating the dielectric constants of these structures. The dielectric constants of the tetragonal and cubic phases of HfO₂ were

^{a)}Electronic mail: eric.cockayne@nist.gov.

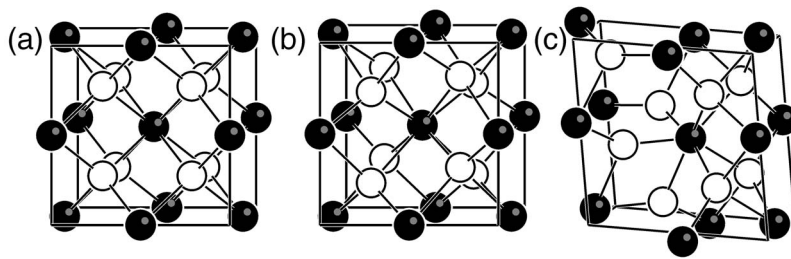


FIG. 1. Three polymorphs of HfO_2 . (a) Cubic high temperature phase. (b) Tetragonal intermediate temperature phase. (c) Monoclinic low temperature phase. Hf are black and O are white.

found to be higher than that of the monoclinic phase^{15–17} providing a natural explanation of how the formation of these phases by ionic substitution in HfO_2 could raise the permittivity. On the other hand, the issues of tetragonal and cubic phase metastability makes it worthwhile to explore whether the permittivity can be increased within the monoclinic phase, for example, by substituting more polarizable ions for Hf.

This work uses first principles calculations to address (1) whether ionic substitution in HfO_2 can make the tetragonal or cubic phase of HfO_2 stable relative to the monoclinic phase, or whether the monoclinic phase remains the most stable, (2) the relative importance of ionic polarizability, local structure, and global symmetry on the dielectric permittivity of HfO_2 with ionic substitutions, and (3) whether the substitution of ions into HfO_2 produces infrared or Raman active phonons whose characteristic frequencies could be experimentally detected. For simplicity, this work focuses on substitutions that do not change the total number of atoms, namely Si, Ti, and Zr substitution for Hf, and the substitution of a Ta–N pair for a Hf–O pair.

II. METHODS

Density-functional theory (DFT) electronic structure calculations for total energies, force constants, and Born effective charges were performed using the Vienna *ab initio* simulation package (VASP).^{18,19} A plane wave basis set was used for electronic wave functions. Projector augmented wave (PAW) pseudopotentials were used for Hf, O, and the substitutional ions.^{20,21} The Hf, Ta, Zr, and Ti PAW pseudopotentials included semicore *p* states as valence electrons. The local density approximation (LDA) was used for the exchange-correlation functional. The electronic contribution to the dielectric response κ_{elec} was calculated using the DFT package ABINIT,²² with Hartwigsen–Goedecker–Hutter pseudopotentials,²³ and the LDA.

TABLE I. Solubility of various compounds in monoclinic HfO_2 .

Compounds	Max. solubility	Intermediate compounds(s)	Reference(s)
Al_2O_3	~1% at ~1800 °C	None	30
Y_2O_3	~1% at ~1800 °C	None	31–33
La_2O_3	~2% at ~1700 °C	$\text{La}_2\text{Hf}_2\text{O}_7$	34 and 35
SiO_2	unknown, <10%	HfSiO_4	36
TiO_2	~9% at ~1600 °C	HfTiO_4	37–39
ZrO_2	Complete	None	40
TaON	Unknown, possibly complete	Unknown	

Calculations were performed for various 12, 24, 48, and 96 atom cells or supercells of HfO_2 (Fig. 3) containing one substitution or pair substitution for the case of Ta–N. The dopant concentration is given by x , yielding the chemical formulae $\text{Hf}_{1-x}\text{M}_x\text{O}_2$ for single ion substitution M, and $\text{Hf}_{1-x}\text{Ta}_x\text{O}_{2-x}\text{N}_x$ for Ta (+N) substitution. Full details of the calculations are given in Ref. 24. The calculations were performed at two levels of convergence: relaxations to find (meta)stable structures were performed using a plane wave cutoff energy of 353 eV, an augmentation charge cutoff energy of 1500 eV, and a Monkhorst Pack grid equivalent to a $6 \times 6 \times 6$ grid on a primitive 12-atom HfO_2 cell. Calculations of phonon frequencies and ionic effective charges were done via the frozen phonon method,²⁵ with a 248 eV plane wave cutoff energy, 1050 eV augmentation charge cutoff energy, and a Monkhorst Pack grid equivalent to a $2 \times 2 \times 2$ grid on a primitive HfO_2 cell.

The small cutoff energy for the phonon and effective charge calculations was a necessary tradeoff between speed and accuracy, given the large number of atoms and low symmetry of the largest monoclinic cells. The convergence errors for the lower cutoff energy calculations were tested for pure HfO_2 and determined to be only $\pm 5 \text{ cm}^{-1}$ for phonon frequencies, ± 0.01 for effective charges, and ± 0.05 for κ_{elec} , while the lower precision calculations were about 40 times faster than the higher precision ones.

III. RESULTS

A. Relative stability of phases

For each structure and each substitution, the energies of the cubic, tetragonal, and monoclinic phases were calculated

TABLE II. Crystalline properties of HfO_2 with various atomic substitutions. Only lowest-energy phase is shown for the given substitution and concentration x . Symmetry is symmetry of the parent HfO_2 phase. m =monoclinic and c =cubic. ΔV is the change in volume relative to the parent HfO_2 structure. Coordination is number of anions in the nearest neighbor shell of the substitutional cation.

Substitution	x	Symm.	ΔV (\AA^3)	Coordination
(Pure HfO_2)	0	m	0	7
Si	0.03125	m	-6.10	6
Si	0.25	c	-5.31	4
Ti	0.03125	m	-4.71	7
Ti	0.25	m	-4.70	7
Zr	0.03125	m	+1.84	7
Zr	0.25	m	+1.64	7
(Ta+N)	0.03125	m	-0.82	7
(Ta+N)	0.25	m	-1.32	7
(Pure TaON)	1.00	m	-7.22	7

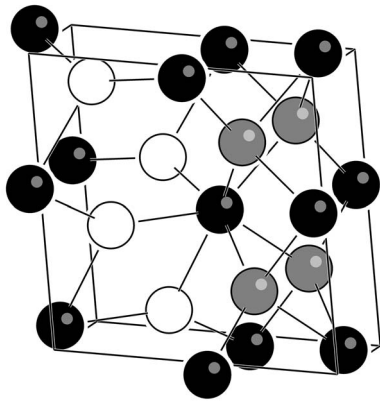


FIG. 2. Monoclinic TaON structure. Ta are black, O white, and N gray.

at various compositions. A HfO_2 supercell was created for each phase, the appropriate ionic substitutions were made, and the structure relaxed. All symmetries are described in terms of the parent HfO_2 phase, although the ionic substitution lowers the symmetry in many cases.

For the simultaneous substitution of a Ta–N pair for a Hf–O pair, many distinct configurations are possible depending upon the distance between the Ta and the N. Figure 4 shows the relative energy of the monoclinic structure as a function of the Ta–N distance. The energy is lowest if N occupies one of the four fourfold O positions nearest to the Ta. The lowest energy is found for N occupying the closest fourfold site. In the remainder of this work, N always replaces the fourfold oxygen closest to Ta.

With Si substitution in the cubic phase, the energy of the system is reduced if four of the neighbors arranged in a tetrahedron moved inward to a distance of 0.160 nm and the other four moved away (see Fig. 5). While tetrahedral oxygen coordination is familiar for Si, similar symmetry breaking, to a lesser degree, lowers the energy for all substitutions tested, except Ta (+N). Remarkably, even the energy of HfO_2 itself is lowered relative to the high symmetry cubic structure of Fig. 1(a) under the distortion of Fig. 5. The tetragonal and distorted cubic structures are related. Phonon analysis of the cubic HfO_2 structure of Fig. 1(a) shows a triplet instability. Freezing one component of this instability gives the tetrago-

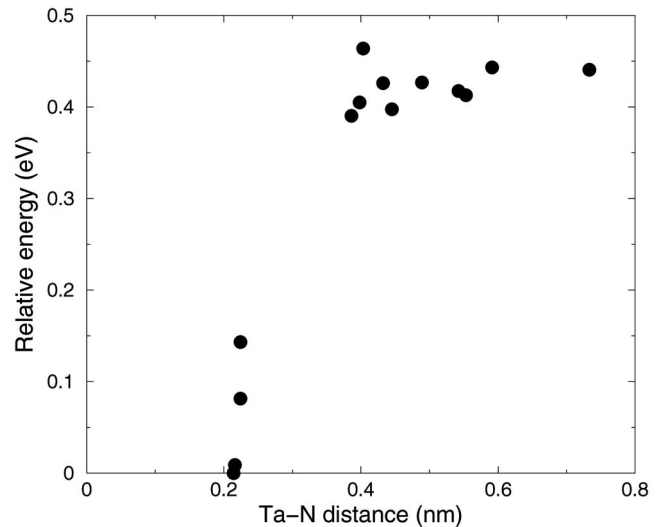


FIG. 4. Calculated relaxed energy of HfO_2 with one Hf and one fourfold coordinated O replaced by Ta and N, respectively, as a function of Ta–N distance.

nal structure of Fig. 1(b) with a select axis c . Freezing a particular superposition of all three components leads to the distorted cubic structure of Fig. 5. For HfO_2 , the ordering of the energies for the system studied, from lowest to highest, is monoclinic, tetragonal, distorted cubic, and high-symmetry cubic. The monoclinic, tetragonal, and high-symmetry cubic phases are in the same order as expected from experiment. Unlike the high-symmetry cubic structure, the tetragonal and distorted cubic structures are metastable, i.e., while they are not ground state structures, normal mode analysis shows that all of their modes are stable.

At sufficiently high concentrations, substitution of small Si or Ti cations stabilizes the distorted cubic structure with respect to the tetragonal one. Because of the complicated competition between cubic, distorted cubic, and tetragonal phases upon ionic substitution, this work reports only the energy differences between the monoclinic phase and the lowest-energy nonmonoclinic phase found as a function of composition. As shown in Fig. 6, ionic substitution lowers the gap in energy between the monoclinic and nonmono-

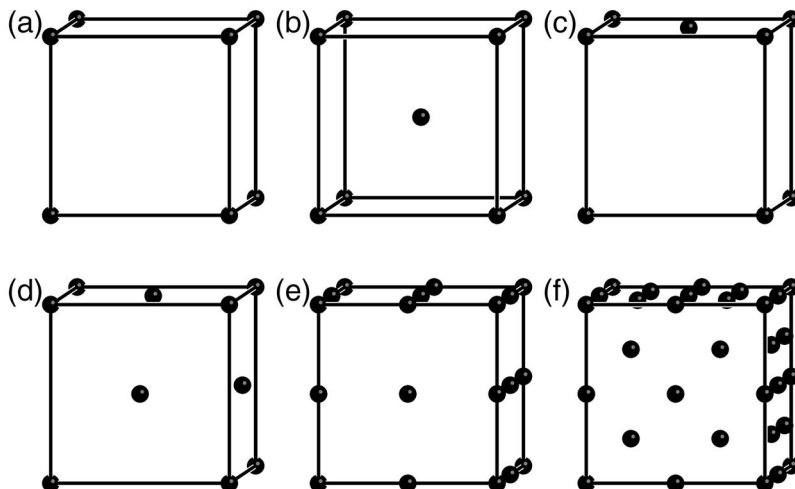


FIG. 3. Arrangements of dopant cations considered. Only the dopant cations are shown, on a common 96-atom supercell of the high-symmetry cubic HfO_2 phase for clarity. (a) $x=0.03125$, (b and c) $x=0.0625$, (d) $x=0.125$, (e) $x=0.25$, and (f) $x=1$. All of the distributions shown are the most uniform and isotropic for a given dopant concentration x , except for (c), which is intentionally chosen to be anisotropic.

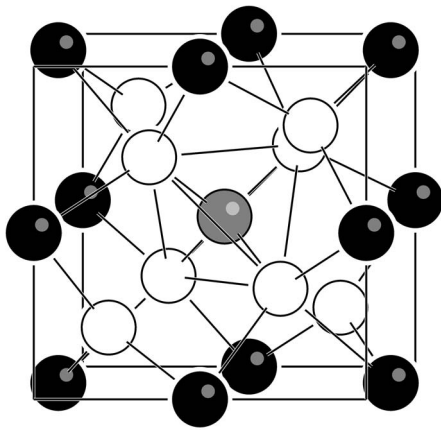


FIG. 5. Distorted cubic $\text{Hf}_{0.75}\text{Si}_{0.25}\text{O}_2$ structure. Hf are black, Si gray, and O white. The cubic coordination of the fluorite structure is broken into a near-neighbor tetrahedron and a second neighbor tetrahedron.

clinic phases for all substitutions studied. Only for Si substitution above about 20%, however, is the lowest nonmonoclinic phase actually stabilized relative to the monoclinic phase. As these results involve the competition between phases of significantly different volume, significant quantitative errors are possible due to the local density approximation. Nonetheless, it is concluded that most experimental studies where ionic substitution produces the tetragonal or cubic phase have either formed a structurally metastable phase or else the nonmonoclinic phase is stabilized by some other factor such as epitaxial strain.

B. Electronic and dielectric properties

Table III lists the LDA band gap, average squared Born effective charge \overline{Z}^{*2} , total static dielectric constant κ_s and the electronic and ionic contributions to κ_s , $\kappa_s = \kappa_{\text{elec}} + \kappa_{\text{ion}}$. The scalar dielectric constant κ_s is defined as $\kappa_s = 1/3 \text{Tr } \boldsymbol{\kappa}_s$, where $\boldsymbol{\kappa}_s$ is the full dielectric tensor. The average squared Born effective charge is defined as the invariant $\overline{Z}^{*2} = 1/(3N) \sum_i \text{Tr}[(\mathbf{Z}_i^*)^T \cdot \mathbf{Z}_i^*]$, where \mathbf{Z}_i^* is the Born effective charge tensor for ion i and the sum runs over the N ions of the unit cell. The results are presented for all of the atomic substitutions at concentrations $x=0.03125$ and $x=0.25$, as

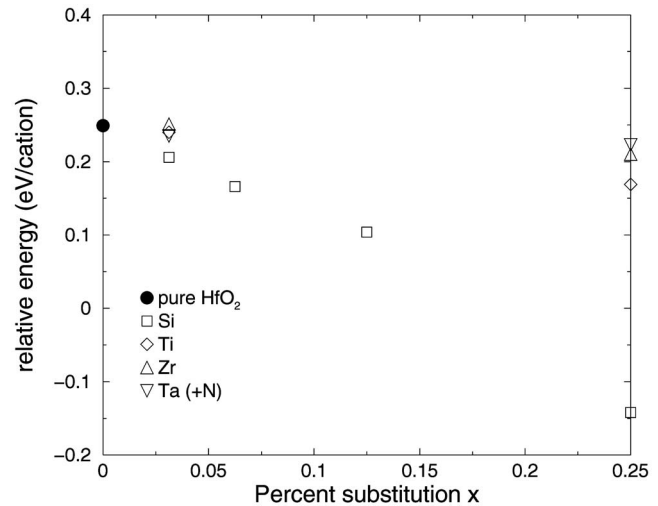


FIG. 6. Energy of lowest-energy nonmonoclinic phase of HfO_2 relative to energy of monoclinic HfO_2 upon ionic substitution and relaxation.

well as for pure TaON. κ_{ion} is related to the phonon properties and Born effective charges of the ions.²⁶ The relationship is expressed here in the simplified form

$$\kappa_s = \kappa_{\text{elec}} + \frac{\overline{Z}^{*2}}{VC}, \quad (1)$$

where V is the volume per ion and C is proportional to the average force constant in the structure weighted appropriately.

Consider first the effects of small dopant concentration. Substitution of Zr for Hf has very little effect, which is not surprising, given the chemical similarities between Zr and Hf. The other ions studied are less similar to Hf, and can be arranged, in order of increasing polarizability, as Si, Hf, Ti, and Ta. The relative polarizabilities of the different ions are consistent with the results in Table III. As the polarizability increases, κ_{elec} and \overline{Z}^{*2} increase. Nonetheless, the total κ_s is increased at $x=0.03125$ whether Si, Ti, or Ta (+N) are substituted. From Eq. (1), it can be concluded that the addition of Si to HfO_2 decreases the volume and softens the lattice enough to more than make up for its smaller polarizability.

More significant changes in κ_s occur when the dopant concentration is higher. The highest κ_s is predicted for mono-

TABLE III. Electronic and dielectric properties of HfO_2 with various atomic substitutions. In some cases, the components of κ_s do not appear to correctly add due to roundoff error.

Substitution	x	LDA band gap (eV)	\overline{Z}^{*2}	κ_{elec}	κ_{ion}	κ_s
(Pure HfO_2)	0	4.04	13.68	4.9	11.6	16.5
Si	0.03125	4.01	13.48	4.9	12.2	17.1
Si	0.25	4.38	12.11	4.8	13.7	18.6
Ti	0.03125	3.08	13.75	5.0	11.9	16.9
Ti	0.25	2.90	14.35	5.2	14.2	19.5
Zr	0.03125	4.00	13.70	4.9	11.6	16.5
Zr	0.25	3.83	13.94	5.0	11.6	16.5
Ta(+N)	0.03125	3.69	13.92	5.1	11.8	16.9
Ta(+N)	0.25	2.95	15.92	5.6	13.5	19.1
(Pure TaON)	1.00	3.01	22.25	8.3	16.4	24.8

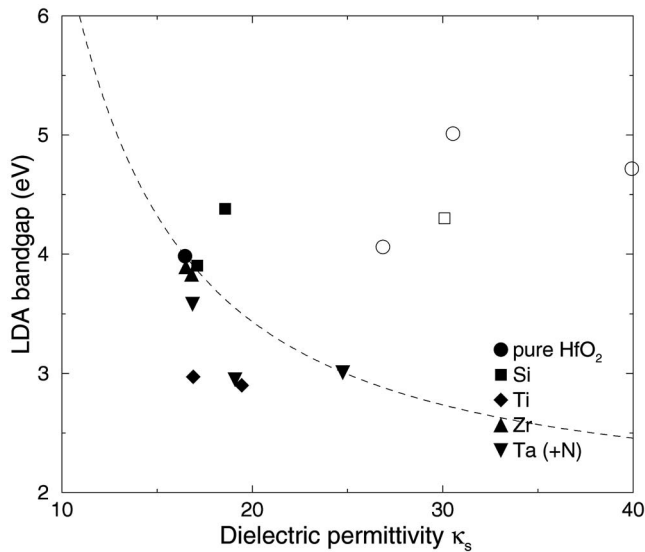


FIG. 7. Local density approximation band gap vs κ_s for HfO_2 and HfO_2 with atomic substitutions. All structures on and below the trendline are based on the monoclinic HfO_2 structure, while those above are based on the tetragonal or cubic HfO_2 structure. Solid symbols represent configurations that are structurally stable. Open symbols are calculated to be metastable with respect to a structural transformation to the monoclinic structure.

clinic TaON, about 1.5 times larger than that of monoclinic HfO_2 . The band gaps of the various structures were also calculated. In Fig. 7, κ_s is plotted against the calculated band gap. It is well known that the local density approximation, which is used here, systematically underestimates the band gap. For example, the experimental band gap²⁷ for HfO_2 is 5.7 eV, versus the calculated value of 4.0 eV in Table III. Nonetheless, one expects the trends in the band gap among related structures to be correctly reproduced. In Fig. 7, the dashed line is the trendline of the maximum dielectric constant for a given band gap, for structures based on the monoclinic phase of HfO_2 . The band gap decreases as κ_s increases (the same trend is observed among oxides in general^{2,28,29}).

This is potentially a problem, as decreasing the band gap of a gate dielectric is detrimental to maintaining sufficient band offsets. For certain ionic substitutions, the band gap is inherently lowered by the electronic states of the substitutional ion. The highest valence band states in HfO_2 are oxygen $2p$ -like and the lowest conduction band states are Hf d -like. When Ti is substituted, the lowest conduction band states become Ti d -like. When Ta and N are substituted, the lowest conduction band states are Ta d -like and the highest valence band states have significant N $2p$ character. Of the ions studied, only Si substitution has little effect on the band gap, as the Si–O bonding states lie well below the valence band maximum and Si–O antibonding states lie well above the conduction band minimum.

The one structure of Table III that increases both the dielectric constant and the band gap relative to HfO_2 is $\text{Hf}_{0.75}\text{Si}_{0.25}\text{O}_2$. This structure differs from the others in that it is cubic, not monoclinic. To better understand how the change in phase from monoclinic to higher symmetry affects the dielectric properties of HfO_2 -based systems, additional calculations were performed on the higher-symmetry polymorphs of HfO_2 . The results are shown in Table IV. The calculated increase in κ_s from monoclinic to cubic to tetragonal agrees with previous reports,^{15,17} as does the finding that the permittivity of tetragonal HfO_2 is smallest along the c axis. In addition, results are presented for HfO_2 with a 12 atom unit cell and the distorted cubic structure shown in Fig. 5. The calculated dielectric constant of this phase is intermediate between that of the cubic and tetragonal phases. Table IV shows that increasing the symmetry of HfO_2 increases the band gap, lowers the average Born effective charge, and has little effect on κ_{elec} . From Eq. (1), the enhancement of κ_s must thus be due to a softer lattice.

These results support the typical experimental observation that the enhancement of dielectric constant of HfO_2 with the addition of dopants is due to the formation of the tetragonal or cubic phase. Tomida, Kita, and Toriumi⁹ (TKT) shows clear x-ray diffraction evidence for the formation of a tetragonal phase in $\text{Hf}_{1-x}\text{Si}_x\text{O}_2$, $0.04 < x < 0.10$, and a maximum dielectric constant $\kappa_s \approx 27$. This presents a puzzle, as first principles total energy calculations show that $\text{Hf}_{1-x}\text{Si}_x\text{O}_2$ at $x=0.0625$ should transform from the tetragonal to four-coordinated cubic phase with no energy barrier. This discrepancy could be resolved if the distribution of Si is not isotropic. Therefore, dielectric calculations were performed on $\text{Hf}_{1-x}\text{Si}_x\text{O}_2$ at $x=0.0625$ with the nonisotropic distribution of Si-rich layers alternating with Hf-only layers shown in Fig. 3(c). The results (Table IV) show (1) that the metastable nonmonoclinic structure has tetragonal symmetry (calculated $c/a=1.009$ versus calculated $c/a=1.016$ for tetragonal HfO_2) and (2) that its calculated dielectric constant 30 is in very good agreement with the TKT experimental result. Such layered structures with alternating Hf-rich and Hf-poor planes are expected when the experimental procedure consists of the alternating atomic layer deposition of HfO_2 and other metal oxides.⁴

In calculating κ_{ion} , the phonon properties were determined for all of the structures studied. The infrared spectra were calculated and Raman spectra estimated as described in Ref. 24. For the most part, the results show only subtle changes in the spectra when ions are substituted within the monoclinic HfO_2 phase. The spectra become very different when the symmetry becomes tetragonal or monoclinic. In one case, an additional peak is predicted, in $\text{Hf}_{1-x}\text{Ta}_x\text{O}_{2-x}\text{N}_x$,

TABLE IV. Structural, electronic, and dielectric properties of metastable HfO_2 phases and anisotropic metastable $\text{Hf}_{0.9375}\text{Si}_{0.0625}\text{O}_2$.

Substitution	x	Symm.	Coordination	LDA band gap (eV)	Z^*2	κ_{elec}	κ_{ion}	κ_s	$(\kappa_s)_{xx}$	$(\kappa_s)_{zz}$
(Pure HfO_2)	0	c	8	4.06	15.22	4.9	22.0	26.9		
(Pure HfO_2)	0	c	4+4	4.46	14.49	5.0	24.8	29.8		
(Pure HfO_2)	0	t	4+4	4.72	14.37	5.0	34.9	39.9	50.6	18.4
Si	0.0625	t	4	4.30	13.69	5.0	25.1	30.1	34.0	22.2

a Raman active mode is predicted at about 828 cm^{-1} due to a stiff bond between a nearest neighbor Ta–N pair. While in the other cases studied, the dopant metal–oxygen bonds have also have characteristic resonance frequencies, these frequencies fall within the broad phonon bands of HfO_2 and, thus, do not remain localized.

IV. CONCLUSIONS

To enhance the dielectric constant of HfO_2 by ionic substitution without significantly decreasing the band gap, the cubic or tetragonal phase must be formed. Of the ionic substitutions studied here, Si is the most intriguing as it is the only one case found where a sufficiently large dopant concentration ($x > \approx 0.2$) is calculated to stabilize a nonmonoclinic phase relative to the monoclinic phase. Otherwise, the nonmonoclinic phases of HfO_2 with atomic substitutions reported experimentally are conjectured to be (1) metastable with respect to the monoclinic phase but with an energy barrier to transformation, (2) stabilized by extrinsic effects such as epitaxial strain or grain boundaries, or (3) stabilized by an configuration of deposited atoms that has a more extreme alternation between Hf-rich and Hf-poor regions than was studied in this work.

The same caveats about *structural* metastability apply to *compositional* metastability. As noted in Table I, the intrinsic solubility of many metal oxides into the monoclinic HfO_2 structure is very small. This does not mean that structurally and/or compositionally metastable structures cannot be made, or that they are useless, but they must satisfy the requirement of not transforming or decomposing over the lifetime of any device in which they are used. The factors that influence the relative stability of these “higher- κ ” phase are a worthwhile area for further research.

- ¹G. D. Wilk, R. M. Wallace, and J. M. Anthony, *J. Appl. Phys.* **18**, 5243 (2001).
²D. G. Schlom and J. H. Haeni, *MRS Bull.* **27**, 198 (2002).
³J. Robertson, *Eur. Phys. J.: Appl. Phys.* **28**, 265 (2004).
⁴P. K. Park and S. W. Kang, *Appl. Phys. Lett.* **89**, 192905 (2006).
⁵E. Rauwel, C. Dubourdieu, B. Holländer, N. Rochat, D. Ducroquet, M. D. Rossell, G. V. Tendeloo, and B. Pelissier, *Appl. Phys. Lett.* **89**, 012902 (2006).
⁶Z. K. Yang, W. C. Lee, Y. J. Lee, P. Chang, M. L. Huang, M. Hong, C.-H. Hsu, and J. Kwo, *Appl. Phys. Lett.* **90**, 152908 (2007).
⁷Y. Yamamoto, K. Kita, K. Kyuno, and A. Toriumi, *Appl. Phys. Lett.* **89**, 032903 (2006).
⁸S. Govindarajan, T. S. Böske, P. Sivasubramani, P. D. Kirsch, U. Schröder, S. Ramanathan, and B. E. Gnade, *Appl. Phys. Lett.* **91**, 062906 (2007).
⁹D. G. Schlom and J. H. Haeni, *Appl. Phys. Lett.* **89**, 142902 (2006).
¹⁰D. H. Triyoso, R. I. Hegde, S. Zollner, M. E. Ramon, S. Kalpat, R. Gregory, X.-D. Wang, J. Jiang, M. Raymond, R. Rai, D. Werho, D. Roan, B.

- E. White, Jr., and P. J. Tobin, *J. Appl. Phys.* **98**, 054104 (2005).
¹¹R. I. Hegde, D. H. Triyoso, S. B. Samavedam, and J. B. E. White, *J. Appl. Phys.* **101**, 074113 (2007).
¹²X. Yu, M. Yu, and C. Zhu, *IEEE Trans. Electron Devices* **54**, 284 (2007).
¹³*Phase Equilibria Diagrams Database v.3.1.0, NIST SRD 31* (The American Ceramic Society, Westerville, OH, 2005).
¹⁴D. Armytage and B. E. F. Fender, *Acta Crystallogr.* **B30**, 809 (1974).
¹⁵X. Zhao and D. Vanderbilt, *Phys. Rev. B* **65**, 233106 (2002).
¹⁶V. Fiorentini and G. Gulleri, *Phys. Rev. Lett.* **89**, 266101 (2002).
¹⁷G. M. Rignanesse, X. Gonze, G. Jun, K. Cho, and A. Pasquarello, *Phys. Rev. B* **69**, 184301 (2004).
¹⁸G. Kresse and J. Furthmüller, *Phys. Rev. B* **54**, 11169 (1996).
¹⁹Certain commercial software is identified in this paper to adequately describe the methodology used. Such identification does not imply recommendation or endorsement by the National Institute of Standards and Technology, nor does it imply that the software identified is necessarily the best available for the purpose.
²⁰P. E. Blochl, *Phys. Rev. B* **50**, 17953 (1994).
²¹G. Kresse and D. Joubert, *Phys. Rev. B* **59**, 1758 (1999).
²²X. Gonze, J.-M. Beuken, R. Caracas, F. Detraux, M. Fuchs, G.-M. Rignanesse, L. Sindic, M. Verstraete, G. Zerah, F. Jollet, M. Torrent, A. Roy, M. Mikami, P. Ghosez, J.-Y. Raty, and D. C. Allen, *Comput. Mater. Sci.* **25**, 478 (2002).
²³C. Hartwigsen, S. Goedecker, and J. Hutter, *Phys. Rev. B* **58**, 3641 (1998).
²⁴E. Cockayne, *Phys. Rev. B* **75**, 094103 (2007).
²⁵O. Zakharov and M. L. Cohen, *Phys. Rev. B* **52**, 12572 (1995).
²⁶E. Cockayne and B. P. Burton, *Phys. Rev. B* **62**, 3735 (2000).
²⁷M. Balog, M. Shieber, M. Michiman, and S. Patai, *Thin Solid Films* **41**, 247 (1977).
²⁸In the notation of Eq. (1), a smaller bandgap increases κ_{elec} because the electronic structure is more easily polarized. Increasing κ_{elec} tends to increase the magnitude of the Z^* due to the increase in the electronic response to an ionic displacement [see, e.g., Ghosez *et al.* (Ref. 29)]. Empirically, the differences in atomic volume and typical interatomic force constant between different simple oxides tend to be relatively small; to a first approximation the denominator VC can be viewed as fixed. Therefore, both the electronic and ionic contributions to κ_s increase as the band gap decreases, all else being equal.
²⁹P. Ghosez, J.-P. Michenaud, and X. Gonze, *Phys. Rev. B* **58**, 6224 (1998).
³⁰L. M. Lopato, A. V. Shevchenko, and G. I. Gerasimiyuk, *Izv. Akad. Nauk SSSR, Neorg. Mater.* **12**, 1331 (1976).
³¹F. M. Spiridonov, L. N. Komissarova, A. G. Kocharov, and V. I. Spitsyn, *Zh. Neorg. Khim.* **14**, 1332 (1969).
³²A. M. Gavrish, B. Y. Sukharevskii, E. I. Zoz, and A. E. Solov'eva, *Izv. Akad. Nauk SSSR, Neorg. Mater.* **9**, 260 (1973).
³³A. V. Shevchenko, L. M. Lopato, and I. E. Kir'yakova, *Izv. Akad. Nauk SSSR, Neorg. Mater.* **20**, 1991 (1984).
³⁴P. Duran, *Ceramurgia Int.* **1**, 10 (1975).
³⁵A. V. Shevchenko, L. M. Lopato, and Z. A. Zaitseva, *Izv. Akad. Nauk SSSR, Neorg. Mater.* **20**, 1530 (1984).
³⁶V. N. Parfenenkov, R. G. Grebenshchikov, and N. A. Toropov, *Dokl. Akad. Nauk SSSR* **185**, 840 (1969).
³⁷R. Ruh, G. W. Hollenberg, E. G. Charles, and V. A. Patel, *J. Am. Ceram. Soc.* **59**, 495 (1976).
³⁸A. V. Shevchenko, L. M. Lopato, I. M. Maister, and Z. A. Zaitseva, *Izv. Akad. Nauk SSSR, Neorg. Mater.* **16**, 1450 (1980).
³⁹J. Coutures, H. W. King, A. M. Lejus, P. Nicholson, P. Odier, and V. Loc, *High Temp. - High Press.* **13**, 97 (1981).
⁴⁰R. Ruh, H. J. Garrett, R. F. Domagala, and N. M. Tallan, *J. Am. Ceram. Soc.* **51**, 23 (1968).